Published in final edited form as:
Cancer Immunol Res. 2013 December ; 1(6): 393–401. doi:10.1158/2326-6066.CIR-13-0109.

CD8+ T Cell Responses Rapidly Select for Antigen-negative Tumor Cells in the Prostate

S. Peter Bak[*,1], **Mike Stein Barnkob**[*,1], **K. Dane Wittrup**[*,‡,§], and **Jianzhu Chen**[*,†]

[*]Koch Institute for Integrative Cancer Research, Massachusetts Institute of Technology, Cambridge, MA 02139, USA

[†]Department of Biology, Massachusetts Institute of Technology, Cambridge, MA 02139, USA

[‡]Department of Biological Engineering, Massachusetts Institute of Technology, Cambridge, MA 02139, USA

[§]Department of Chemical Engineering, Massachusetts Institute of Technology, Cambridge, MA 02139, USA

Abstract

Stimulation of patients' immune systems for the treatment of solid tumors is an emerging therapeutic paradigm. The use of enriched autologous T cells for adoptive cell therapy (ACT) or vaccination with antigen-loaded dendritic cells have shown clinical efficacy in melanoma and prostate cancer, respectively. However, the long-term effects of immune responses on selection and outgrowth of antigen-negative tumor cells in specific tumor types must be determined in order to understand and achieve long term therapeutic effects. In this study, we have investigated the expression of a tumor specific antigen *in situ* after treatment with tumor specific $CD8^+$ T cells in an autochthonous mouse model of prostate cancer. After T cell treatment, aggregates of dead antigen-positive tumor cells were concentrated in the lumen of prostate gland and were eventually eliminated from the prostate tissue. Despite the elimination of antigen-positive tumor cells, prostate tumor continues to grow in T cell treated mice. Interestingly, remaining tumor cells were antigen-negative and downregulated MHC class I expression. These results show that $CD8^+$ T cells are effective in eliminating antigen-bearing prostate tumor cells but they also can select for the outgrowth of antigen-negative tumor cells. These findings provide insights into the requirements for an effective cancer immunotherapy within the prostate: not only inducing potent immune responses but also avoiding selection and outgrowth of antigen-negative tumor cells.

Keywords

Prostate Cancer; T Cells; Adoptive Cell Therapy; Immunoediting; Tumor Antigens

Address correspondence and reprint requests to Jianzhu Chen, Koch Institute for Integrative Cancer Research, Massachusetts Institute of Technology, 76-261A, Cambridge, MA 02139. Tel: 617-258-6173, FAX: 617-258-6172, jchen@mit.edu.

[1]Authors contributed equally to this work

Conflict of Interest: None

Introduction

A promising cancer immunotherapy is induction of tumor antigen specific $CD8^+$ T cell responses. An autologous dendritic cell vaccine targeting prostate acid phosphatase has recently been approved for the treatment of metastatic castration resistant prostate cancer (1). Adoptive cell therapy (ACT), which harvests tumor infiltrating T lymphocytes (TILs), expands them *ex vivo*, and introduces the expanded T cells back to the patient (2), is being developed for treatment of melanoma where strong tumor associated antigens have been described (3). Despite the enormous promise, one potential drawback of antigen-specific cancer immunotherapy is the selection and outgrowth of antigen-negative tumor cells, which can render the immunotherapy ineffective.

Most studies that have examined the selection and outgrowth of antigen-negative tumor cells following induction of tumor-specific $CD8^+$ T cell responses have been carried out in animal models. For example, the PA14 antigen (PA14) has been introduced into different tumors, including mastocytomas, plasmocytomas, and fibrosarcomas. When these tumors were transplanted into recipient mice followed with ACT with PA14-specific T cells, antigen loss and tumor outgrowth was observed in all tumor types (4). Similarly, when ovalbumin (OVA)-expressing B16 melanoma cells were transplanted into recipient mice followed with treatment with OVA specific OT-1 $CD8^+$ T cells, downregulation of OVA expression was also detected (5, 6). The downregulation of target antigen is not limited to model antigens that were overexpressed in tumor cells. Vaccination of mice transplanted with B16 melanomas induced $CD8^+$ T cell responses that selected for tumor cells with downregulated expression of tyrosinase and tyrosinase-related protein 2 antigens (7), suggesting that expression of endogenous tumor antigens are also subject to inhibition as a result of anti-tumor immune responses.

The ability of immune responses to sculpt the antigen repertoire of spontaneously arising tumors is less clear. In a genetically engineered model of melanoma, targeting the gp100 protein with tumor specific T cells led to de-differentiation of melanocytes with concurrent loss of the gp100 antigen (8). Another widely studied autochthonous tumor model is the transgenic adenocarcinoma of the mouse prostate (TRAMP) as a result of prostate-specific expression of the SV40 large T antigen (Tag). Numerous studies have examined the effect of immunotherapies on TRAMP tumor growth because of the potential of immunotherapy in treating human prostate cancer. However, there has been little analysis on the effect of T cells on antigen expression within TRAMP tumors, and the ability of T cells to select antigen loss variants. A recent study examined the ability of anti-HA T cells to control the growth of prostate tumor in TRAMP mice engineered to express the HA antigen (9). While tumor growth was assessed by prostate weight and histology, there was no examination of antigen expression in the prostate. Similarly, a telomerase vaccine was tested in the TRAMP model and shown to exhibit a protective effect, despite eventual tumor outgrowth (10). While T cell responses, prostate tumor histopathology, and total survival were measured, there was no post-vaccination measurement of target antigen expression (10). Additional studies evaluating the effect of anti-Tag T cells on TRAMP tumors have assessed tumor burden, but have not assessed levels of Tag protein *in situ* (11, 12). As such, a clearer understanding of immunoediting beyond transplantable and melanoma models is needed.

In our study of $CD8^+$ T cell-tumor cell interaction, we have introduced a β-gal-SIY transgene encoding a fusion protein of β-galactosidase with a nominal MHC class I epitope (SIYRYYGL or SIY) recognized by the 2C clonotypic TCR onto the TRAMP mice (TRP-SIY) (13). Adoptive transfer of naïve $CD8^+$ 2C T cells into TRP-SIY mice followed by infection with influenza virus expressing the SIY epitope leads to activation and differentiation of transferred T cells into potent effector cells. As in human patients, effector T cells infiltrate into the prostate tumor tissue and are rapidly tolerized. Similar to human TILs, the 2C T cells persist in the prostate tumor tissue (14) and express high levels of PD-1 (15). This system provides a tractable model to study in detail the effects of adoptively transferred T cells on tumor specific antigen expression. Here, we show that infiltration of activated 2C T cells into the prostate leads to elimination of SIY-positive tumor cells. However, tumor in the prostate of 2C T cell-treated TRP-SIY mice continues to progress with similar kinetics as that in untreated mice. A detailed analysis reveals that all tumor cells in the treated mice are negative for SIY antigen and have also downregulated MHC class I expression. These findings show that $CD8^+$ T cells are effective in eliminating antigen-bearing prostate tumor cells but they also select for the outgrowth of antigen-negative tumor cells. These findings shed light on effective cancer immunotherapy that requires not only inducing potent immune responses but also avoiding selection and outgrowth of antigen-negative tumor cells.

Materials and Methods

Mice, Adoptive Transfer and Influenza Infection

TRP-SIY mice were generated as previously described (13). 2C and OT-1 TCR transgenic mice were maintained on C57BL/6 and $RAG1^{-/-}$ backgrounds. Where indicated, 16 week-old mice were retroorbitally injected with 1.5×10^6 naïve 2C or OT-1 cells from 2C/RAG or OT-1/RAG mice and immediately infected intranasally with 100 pfu WSN-SIY or WSN-SIIN virus, respectively. T cell treated and WSN infected mice were paired with aged matched control mice where indicated. Experiments with mice were approved by the Committee on Animal Care (CAC) at Massachusetts Institute of Technology.

Immunohistochemistry

At indicated time points after T cell treatment, the genitourinary tract was excised and all four prostate lobes dissected and flash frozen in OCT compound (Tissue-Tek, Sakura). All tissues were sectioned to 10 μM by the Koch Institute Histology core facility along with matched hematoxylin and eosin (H&E) stained slides. For immunohistochemistry, frozen sections were acetone fixed, blocked with 0.3% H2O2 in PBS. Staining was conducted with Vectastain Elite ABC kit (Vector Laboratories) according to the manufacturer's instructions. In some instances slides were stained with X-gal solution (5mM potassium ferricyanide, 2mM magnesium chloride, 1mg/mL X-gal stock solution (Promega) in PBS) for three hours before incubation with primary antibody. Biotinylated antibodies against Thy1.1 (clone HIS51, eBioscience), MHC class I (clone 28-8-6 BD Pharmingen), and CD31 (clone MEC13.3, BioLegend) were visualized with DAB peroxidase staining kit (Vector Labs). Anti-SV40 large T antigen (clone Pab 101, BD Bioscience) staining was conducted with Vectastain Mouse on Mouse Peroxidase Kit (Vector Laboratories), according to the

manufacturer's instructions. Where indicated slides were counterstained with eosin (Sigma) or hematoxylin (Vector Labs).

Image and Pathological Analysis

For image analysis, 10 random images were acquired for each sample representing all prostate glands on Zeiss Axioplan II with 10X or 40X objective. For whole mount images, a MIRAX Midi (Carl Zeiss) slide scanner with Axiocam MR(m) camera (Carl Zeiss) was used and images captured using the MIRAX Viewer Software (Carl Zeiss). Peroxidase or β-gal staining was visualized on each image by thresholding and using preset protocols in Volocity 6.01 (PerkinElmer), such that a precise measurement of area could be made. Total area of gland was determined based on eosin or hematoxylin staining. Contact between stains, as well as luminal and glandular measurements were individually outlined in Volocity and then measured using the preset protocols as above. H&E stained prostate lobes were blindly graded by Dr. Roderick Bronson at the Koch Institute for Integral Cancer Research Pathology Core Facility using the following scale: 0, normal tissue; 1, proliferation with no invasion; 2, early invasion; 3, clear-cut invasion; 4, total replacement of organ.

Statistical Analysis

Data was analyzed with Prism 5.0 (GraphPad Software). Student *t* test was used for comparisons. A p value of less than 0.05 was considered statistically significant. In figures * is indicative of $p < 0.05$, ** $p < 0.01$ and *** $p < 0.001$. Bar graphs represent mean ± standard deviation (SD).

Results

Prostate infiltrating T cells gradually lose contact with antigen-expressing tumor cells

To determine the localization of tumor infiltrating T cells relative to antigen expressing cells in the prostate tumor tissue, we developed an immunohistochemistry analysis for 2C T cells by staining for Thy1.1 (brown) and antigen (SIY)-expressing cancer cells by X-gal staining (blue) for β-galacatosidase (β-gal) in the prostate tumor tissue. In agreement with previous flow cytometry analysis (13), $Thy1.1^+$ 2C T cells were found in the prostate gland 11 days post transfer and infection (dpt) (Fig. 1A). Eleven dpt was chosen as an initial time point because 2C T cell infiltration into the TRP-SIY prostates starts 7 dpt and reaches the peak level around 10 dpt (13). To quantify the Thy1.1 signal, we determined the total area stained by Thy1.1 as a function of the total glandular area stained by eosin (Fig. 1B). Thy1.1 staining area (level) covered approximately 10% of the prostate tumor tissue 11 dpt (Fig. 1B). However, by 35 to 50 dpt, the levels of 2C T cell staining decreased by 75%. These results match the kinetics of T cell levels in TRP-SIY prostates as quantified by flow cytometry analysis of dissociated tissues (13).

To determine whether 2C T cells were in contact with antigen-expressing tumor cells in the prostate tumor, $Thy1.1^+$ staining was separated into categories based on relative distance from the antigen (β-gal) staining. Contiguous staining of Thy1.1 and β-gal was considered as direct contact between 2C T cells and SIY-expressing tumor cells (Fig. 1C, center top). Thy1.1 signal was further categorized into staining within antigen positive glands but not in

direct contact with antigen (Fig. 1C, top right), staining within antigen negative glands (Fig. 1C, lower left), staining outside of the glandular area in the interstitial space (Fig. 1C, center bottom), and staining within the luminal space of the prostate gland (Fig. 1C, lower right). We used this analysis to quantify the changes of 2C T cells within the prostate at 11, 35 and 50 dpt and expressed each category as a fraction of total Thy1.1 signal across the three time-points (Fig. 1D). At 11 dpt approximately 15% of 2C T cells were in direct contact with SIY-expressing cells, with the majority of cells residing within antigen positive prostate glands. By 35 dpt only 5% of 2C T cells were in contact with SIY-expressing cells, although the majority still resided in the antigen positive glands. After 50 dpt, however, very few 2C T cells were in contact with SIY-expressing cells or resided in the antigen positive glands. Associated with the gradual loss of T cell/antigen contact, the proportion of $Thy1.1^+$ 2C T cells in the $\beta\text{-gal}^-$ gland increased. These data show that over time tumor-infiltrating (2C) T cells gradually lose contact with antigen (SIY)-expressing tumor cells in the prostate tissue.

T cell treatment leads to loss of antigen-expressing tumor cells in the prostate

To determine whether the decrease in T cell/antigen contact within the prostate tissue was due to loss of antigen expression over time, we harvested prostate tissues from age-matched TRP-SIY mice with (treated) or without (untreated) 2C T cell transfer/infection, stained tissue sections for β-gal and quantified the percentage of β-gal staining as a function of total prostate glandular area. TRP-SIY prostates normally contain large areas of epithelia that stained positive for β-gal (Fig. 2A, left). Eleven days after 2C T cell treatment, the percentage of β-gal positive areas did not change significantly (Fig. 2A and B). However, by 35 and 50 dpt the level of antigen expression was reduced significantly. The loss of SIY-expressing cells was antigen specific as transfer of OT-1 T cells that recognize SIINFEKL (SIIN) epitope and infection with WSN virus that expresses the SIIN epitope (WSN-SIIN) did not induce the loss of β-gal-expressing cells within the prostates of TRP-SIY mice (Fig. 2B).

We noticed the spatial distribution of X-gal staining was markedly different between untreated and 2C T cell-treated mice 11 dpt. In untreated mice, β-gal staining was spread throughout the prostate tissue (Fig. 2A, top) and over 90% of staining was found in glandular epithelia (Fig. 2C). In contrast, in the treated mice ∼80% β-gal staining was found in the lumen of prostate glands. To determine whether the luminal β-gal positive areas contained viable cells, we compared consecutive sections of tissue stained with either hematoxylin and eosin (H&E) or X-gal. Luminal areas that stained positive for β-gal after T cell treatment were composed of hematoxylin (nuclear stain) negative and eosin positive (cytoskeleton) cellular debris (Fig. 2D). Furthermore, β-gal stains were also detected in the urethra of treated mice (data not shown). These data suggest that the loss of b-gal–expressing tumor cells are likely due to elimination by infiltrating antigen-specific 2C T cells and the mass of dead tumor cells are cleared through the luminal space.

The Presence of 2C T cells within the prostate leads to a reduced expression of MHC class I

Immune responses within the tumor environment can affect antigen expression as well as molecules involved in antigen presentation, particularly MHC class I (16, 17). To determine

if 2C T cell treatment of TRP-SIY mice reduces the MHC I expression within prostate tissue, we stained prostate sections from treated and untreated TRP-SIY mice for MHC I expression (Fig. 3A), and quantified the expression as a fraction of total prostate tissue area (Fig. 3B). Eleven days after 2C T cell treatment MHC I expression in treated mice was higher than that of untreated mice (Fig. 3B). By 35 dpt two of the four treated mice contained a similar percentage of MHC I+ tissue area as untreated mice while the other two mice had much reduced percentage. By 50 dpt only ∼10% of prostate tissue exhibited MHC I staining, as compared to 30-50% of MHC I+ tissue in untreated mice (Fig. 3B, p value of < 0.001). The reduction of MHC I+ expression was largely antigen specific as transfer of OT-1 T cells and infection with WSN-SIIN virus did not affect expression of MHC I expression within the prostates of TRP-SIY mice to the extent of 2C T cells (Fig. 3B). In total, this data indicates that after long term exposure to antigen specific T cells, cell surface expression of MHC I within the prostate epithelium is reduced.

In addition to antigen expression, activated T cells within tumors can disrupt tumor stroma, such as $CD31^+$ endothelial cells (18). We determined the levels of tumor vasculature by staining prostate tissue for CD31. Prostate tissue in TRP-SIY mice were well vascularized with clear CD31 staining in both 2C T cell treated and untreated mice (Fig. 3C). No difference in percentage of area that stained positive for CD31 was detected in untreated and treated mice (Fig. 3D). Together, these data show that 2C T cell response in the prostate tissue leads to a reduction of MHC I expression but not the tumor vasculature.

2C T cell treatment does not alter tumor progression

We next determined whether reduction in antigen expressing prostate cells in treated mice affected tumor progression. To assess tumor progression, H&E stained prostate tissues from 2C treated and untreated mice were blinded and graded for tumor stage (Fig. 4A). At 11 dpt the average tumor grade was the same (1.4) in both treated and age-matched control mice (Fig. 4A). At 35 dpt the average tumor grade in treated and age matched controls was 2.2 and 2.5, respectively. At 50 dpt the average grade was 3.8 for treated mice versus 2.8 for untreated mice. These data suggest that despite clearance of SIY-expressing cells in the TRP-SIY prostates, tumors continue to progress.

To determine why disease score was similar between treated and age matched control mice across various time points, we evaluated the expression of the SIY and the oncogene driving tumor growth in TRP-SIY mice. TRP-SIY mice were constructed by introducing the β-gal-SIY fusion transgene into the TRAMP mice, which carry the SV40 large T antigen (Tag) transgene. Although both transgenes were driven by the same prostate-specific promoter, the two transgenes were introduced into the mouse genome independently. It is possible that activated 2C T cells eliminated SIY-expressing tumors while those that do not express the SIY antigen grow out after T cell treatment. To test this possibility, we stained untreated TRP-SIY prostate sections for both β-gal and Tag. Although most β-gal and Tag staining overlapped, a significant fraction of prostate area was stained positive for Tag but negative for β-gal (Fig. 4B). Furthermore, to assess the expression of the Tag after 2C T cell treatment we stained treated and untreated prostate sections for Tag (Fig. 4C). At all three time points (11, 35 and 50 dpt), the 2C T cell treatment did not affect the percentage of

prostate tissue that stained positive for Tag (Fig. 4D). However, the percentage of Tag-positive area increased over time following 2C treatment, correlating with tumor progression. Taken together, these data suggest that although 2C T cell treatment is effective in eliminating SIY-positive tumor cells, the SIY-negative tumor cells continue to progress.

Discussion

The TRAMP model has been widely used to study prostate cancer immunotherapy. Numerous studies have induced $CD8^+$ T cell responses to TRAMP tumor, including clonotypic $CD8^+$ T cells specific for Tag, HA or SIY epitopes that were engineered to be expressed in the tumor cells, or endogenous $CD8^+$ T cells following immunization with a telomerase vaccine. Although antigen-specific $CD8^+$ T cells were potently induced in each case, the effect on tumor growth is minimal or transient, as the outgrowth of tumor cells eventually kills the TRAMP mice. The lack of long-lasting efficacy has been attributed to the rapid tolerization of tumor infiltrating T cells by the immunosuppressive tumor environment within TRAMP mice (13, 19, 20). In the current study, by quantifying the level and distribution of responding $CD8^+$ T cells and antigen-bearing tumor cells in the prostate, we show that $CD8^+$ T cells are very effective in eliminating antigen-bearing tumor cells in the prostate. One week after infiltration into the prostate tumor tissue, most of antigen-bearing tumor cells are already eliminated. Notably, aggregates of dead antigen-positive tumor cells are found in the lumen of the prostate gland and in the urethra, suggesting that killed tumor cells are removed from the prostate tissue through the lumen and urethra. These findings suggest that $CD8^+$ T cells are more effective than previously realized in eliminating antigen-positive tumor cells in the prostate and alternative mechanisms underlying the lack of efficacy on tumor progression and survival of TRAMP mice as observed in many studies.

Our observation of the selection and outgrowth of antigen-negative tumor cells in TRP-SIY mice provides such a mechanism. We show that while SIY-positive tumor cells are eliminated soon after T cell infiltration into the prostate, SIY-negative but Tag^+ cells continue to grow within the tumor bed. The presence of Tag^+ SIY (β-galactosidase)$^-$ tumor cells in TRP-SIY mice prior to T cell treatment further suggests that the outgrowth of Tag^+ SIY^- tumor cells compromised the efficacy of 2C T cell treatment. This observation is likely an instance of immune-editing where immune responses keep tumors under the control but antigen-negative tumor cells eventually outgrow and escape immune surveillance. Our findings suggest that targeting multiple epitopes in poorly immunogenic tumors may increase the efficacy of immunotherapies. Indeed, in a B16-OVA model where treatment of mice with OT-1 T cells was unable to control tumor growth (6), treatment with both OT-1 and the gp-100 specific Pmel-1 T cells prevented tumor growth (21). Furthermore, our work suggests that targeting of oncogenic drivers of tumor growth with immunotherapy could be a more productive strategy. Previous attempts to use T cells that recognize Tag epitopes in the TRAMP model have provided mixed results with regards to reduction in tumor burden (11, 12). Nevertheless, other models have demonstrated the therapeutic benefit of focusing the immune response toward overexpressed oncogenes, including Tag (18). The efficacy of combination immunotherapies that target oncogene epitopes and non-oncogene epitopes should be investigated in this and other models.

In addition to antigen loss, cell surface expression of MHC I within the prostate epithelium is reduced in mice 50 dpt. The reduction in the percentage of MHC class I area could result from elimination of antigen-expressing tumor cells and/or downregulation of MHC class I expression on the remaining prostate tumor cells. Selection and outgrowth of antigen-negative tumor cells and the lack of effect of clonotypic T cells specific for an irrelevant antigen (OT-1 T cells) on SIY expression in the prostate (Fig. 2B) highlight the first possibility. The modest, yet statistically significant effect of OT-1 T cells on the percentage of MHC class I area (Fig. 3B) would support the second mechanism. While further studies are needed to determine the relative contribution of the two mechanisms, the reduction of MHC class I tumor cells likely contributes to the decreased T-cell/antigen contact 35 and 50 dpt (Fig. 1D). The decrease in T-cell/antigen contact could result from a decreased adhesion of T cells to tumor cells and/or stoichiometric issues due to the loss of antigen-positive tumor cells. Consistent with the first possibility, infiltrating 2C T cells are rapidly tolerized in the prostate tumor environment (13), which may decrease their ability to adhere to tumor cells. By 50 dpt, SIY-expressing tumor cells have been eliminated and the percentage of MHC class I area has reduced significantly (Figs. 2B and 3B), which likely reduce 2C T-cell/antigen contact due to the paucity of antigen-positive cells in the prostate.

In human melanoma, esophageal, and ovarian cancers MHC I loss is associated with poor prognosis (17, 22, 23). Data from human prostate cancers is mixed with regard to MHC I expression. A study assessing patient samples from varying tumor stages (Gleason stages 6-10) found MHC I expression in all cases (24). A more recent study assessed components of the antigen processing machinery in 59 primary prostate carcinoma and prostate carcinoma cell lines. HLA class I was retained in most tumor lesions, but intracellular antigen processing machinery was not detected in at least 21% tumors (16). Regardless, under steady state conditions MHC I cell surface expression is retained in TRAMP tissues (24). The role of immunotherapies on MHC I expression within prostates of human patients is of interest, as MHC I loss can profoundly influence the efficacy of adaptive immune responses.

The long-term effect on antigen expression and antigen loss variants in many immunotherapeutic modalities is unknown. Clinical trials evaluating ACT in relapsing metastatic melanoma patients demonstrate the emergence of antigen loss variants (25-27). However, whether selection for antigen-negative tumor cells also occurs in other tumor types following induction of a therapeutic immune response has yet to be determined. The effect of the FDA approved DC vaccination protocol on antigen expression in primary or relapsing prostate tumors has not been reported. Collectively, these studies will have important implications for the selection of tumor specific antigens and suggest selection of multiple antigens, including those that drive tumor progression, are attractive targets for generating clinical benefit.

Acknowledgments

Grant Support: This work was partly supported in part by a Postdoctoral Fellowship (12109-PF-11-025-01-LIB) from the American Cancer Society (S.P.B.), the Margaret A. Cunningham Immune Mechanisms in Cancer Research Fellowship (S.P.B.) from the John D. Proctor Foundation, a Prostate Cancer Research Program grant from

USAMRMC and Ivan R. Cottrell Professorship and Research Fund (to J.C.), and the Koch Institute Support (core) Grant P30-CA14051 from the National Cancer Institute.

We thank Marisha Mikell and the Swanson Biotechnology Core Facility at the Koch Institute for their technical support, members of the Chen and Wittrup Labs for their helpful discussions, and Yin Lu at the Singapore-MIT Alliance for Research and Technology for assistance with processing histology slides.

References

1. Cha E, Fong L. Immunotherapy for Prostate Cancer: Biology and Therapeutic Approaches. J Clin Oncol. 2011
2. Rosenberg SA, Restifo NP, Yang JC, Morgan RA, Dudley ME. Adoptive cell transfer: a clinical path to effective cancer immunotherapy. Nat Rev Cancer. 2008; 8:299–308. [PubMed: 18354418]
3. Dudley ME, Wunderlich JR, Yang JC, Sherry RM, Topalian SL, Restifo NP, Royal RE, Kammula U, White DE, Mavroukakis SA, Rogers LJ, Gracia GJ, Jones SA, Mangiameli DP, Pelletier MM, Gea-Banacloche J, Robinson MR, Berman DM, Filie AC, Abati A, Rosenberg SA. Adoptive cell transfer therapy following non-myeloablative but lymphodepleting chemotherapy for the treatment of patients with refractory metastatic melanoma. J Clin Oncol. 2005; 23:2346–57. [PubMed: 15800326]
4. Bai XF, Liu JQ, Joshi PS, Wang L, Yin L, Labanowska J, Heerema N, Zheng P, Liu Y. Different lineages of P1A-expressing cancer cells use divergent modes of immune evasion for T-cell adoptive therapy. Cancer Res. 2006; 66:8241–9. [PubMed: 16912204]
5. Goldberger O, Volovitz I, Machlenkin A, Vadai E, Tzehoval E, Eisenbach L. Exuberated numbers of tumor-specific T cells result in tumor escape. Cancer Res. 2008; 68:3450–7. [PubMed: 18451173]
6. Kaluza KM, Thompson JM, Kottke TJ, Flynn Gilmer HC, Knutson DL, Vile RG. Adoptive T cell therapy promotes the emergence of genomically altered tumor escape variants. Int J Cancer. 2012; 131:844–54. [PubMed: 21935923]
7. Sanchez-Perez L, Kottke T, Diaz RM, Ahmed A, Thompson J, Chong H, Melcher A, Holmen S, Daniels G, Vile RG. Potent selection of antigen loss variants of B16 melanoma following inflammatory killing of melanocytes in vivo. Cancer Res. 2005; 65:2009–17. [PubMed: 15753401]
8. Landsberg J, Kohlmeyer J, Renn M, Bald T, Rogava M, Cron M, Fatho M, Lennerz V, Wolfel T, Holzel M, Tuting T. Melanomas resist T-cell therapy through inflammation-induced reversible dedifferentiation. Nature. 2012; 490:412–6. [PubMed: 23051752]
9. Wada S, Yoshimura K, Hipkiss EL, Harris TJ, Yen HR, Goldberg MV, Grosso JF, Getnet D, Demarzo AM, Netto GJ, Anders R, Pardoll DM, Drake CG. Cyclophosphamide augments antitumor immunity: studies in an autochthonous prostate cancer model. Cancer Res. 2009; 69:4309–18. [PubMed: 19435909]
10. Mennuni C, Ugel S, Mori F, Cipriani B, Iezzi M, Pannellini T, Lazzaro D, Ciliberto G, La Monica N, Zanovello P, Bronte V, Scarselli E. Preventive vaccination with telomerase controls tumor growth in genetically engineered and carcinogen-induced mouse models of cancer. Cancer Res. 2008; 68:9865–74. [PubMed: 19047167]
11. Anderson MJ, Shafer-Weaver K, Greenberg NM, Hurwitz AA. Tolerization of tumor-specific T cells despite efficient initial priming in a primary murine model of prostate cancer. J Immunol. 2007; 178:1268–76. [PubMed: 17237372]
12. Shafer-Weaver KA, Watkins SK, Anderson MJ, Draper LJ, Malyguine A, Alvord WG, Greenberg NM, Hurwitz AA. Immunity to murine prostatic tumors: continuous provision of T-cell help prevents CD8 T-cell tolerance and activates tumor-infiltrating dendritic cells. Cancer Res. 2009; 69:6256–64. [PubMed: 19622771]
13. Bai A, Higham E, Eisen HN, Wittrup KD, Chen J. Rapid tolerization of virus-activated tumor-specific CD8+ T cells in prostate tumors of TRAMP mice. Proc Natl Acad Sci U S A. 2008; 105:13003–8. [PubMed: 18723683]
14. Olurinde MO, Shen CH, Drake A, Bai A, Chen J. Persistence of tumor-infiltrating CD8 T cells is tumor-dependent but antigen-independent. Cell Mol Immunol. 2011

15. Bak SP, Barnkob MS, Bai A, Higham EM, Wittrup KD, Chen J. Differential requirement for CD70 and CD80/CD86 in dendritic cell-mediated activation of tumor-tolerized CD8 T cells. J Immunol. 2012; 189:1708–16. [PubMed: 22798683]

16. Seliger B, Stoehr R, Handke D, Mueller A, Ferrone S, Wullich B, Tannapfel A, Hofstaedter F, Hartmann A. Association of HLA class I antigen abnormalities with disease progression and early recurrence in prostate cancer. Cancer Immunol Immunother. 2010; 59:529–40. [PubMed: 19820934]

17. Kageshita T, Hirai S, Ono T, Hicklin DJ, Ferrone S. Down-regulation of HLA class I antigen-processing molecules in malignant melanoma: association with disease progression. Am J Pathol. 1999; 154:745–54. [PubMed: 10079252]

18. Anders K, Buschow C, Herrmann A, Milojkovic A, Loddenkemper C, Kammertoens T, Daniel P, Yu H, Charo J, Blankenstein T. Oncogene-targeting T cells reject large tumors while oncogene inactivation selects escape variants in mouse models of cancer. Cancer Cell. 2011; 20:755–67. [PubMed: 22172721]

19. Watkins SK, Zhu Z, Riboldi E, Shafer-Weaver KA, Stagliano KE, Sklavos MM, Ambs S, Yagita H, Hurwitz AA. FOXO3 programs tumor-associated DCs to become tolerogenic in human and murine prostate cancer. J Clin Invest. 2011; 121:1361–72. [PubMed: 21436588]

20. Donkor MK, Sarkar A, Savage PA, Franklin RA, Johnson LK, Jungbluth AA, Allison JP, Li MO. T cell surveillance of oncogene-induced prostate cancer is impeded by T cell-derived TGF-beta1 cytokine. Immunity. 2011; 35:123–34. [PubMed: 21757379]

21. Kaluza KM, Kottke T, Diaz RM, Rommelfanger D, Thompson J, Vile R. Adoptive transfer of cytotoxic T lymphocytes targeting two different antigens limits antigen loss and tumor escape. Hum Gene Ther. 2012; 23:1054–64. [PubMed: 22734672]

22. Mizukami Y, Kono K, Maruyama T, Watanabe M, Kawaguchi Y, Kamimura K, Fujii H. Downregulation of HLA Class I molecules in the tumour is associated with a poor prognosis in patients with oesophageal squamous cell carcinoma. Br J Cancer. 2008; 99:1462–7. [PubMed: 18841157]

23. Han LY, Fletcher MS, Urbauer DL, Mueller P, Landen CN, Kamat AA, Lin YG, Merritt WM, Spannuth WA, Deavers MT, De Geest K, Gershenson DM, Lutgendorf SK, Ferrone S, Sood AK. HLA class I antigen processing machinery component expression and intratumoral T-Cell infiltrate as independent prognostic markers in ovarian carcinoma. Clin Cancer Res. 2008; 14:3372–9. [PubMed: 18519766]

24. Nanda NK, Birch L, Greenberg NM, Prins GS. MHC class I and class II molecules are expressed in both human and mouse prostate tumor microenvironment. Prostate. 2006; 66:1275–84. [PubMed: 16741922]

25. Thurner B, Haendle I, Roder C, Dieckmann D, Keikavoussi P, Jonuleit H, Bender A, Maczek C, Schreiner D, von den Driesch P, Brocker EB, Steinman RM, Enk A, Kampgen E, Schuler G. Vaccination with mage-3A1 peptide-pulsed mature, monocyte-derived dendritic cells expands specific cytotoxic T cells and induces regression of some metastases in advanced stage IV melanoma. J Exp Med. 1999; 190:1669–78. [PubMed: 10587357]

26. Maeurer MJ, Gollin SM, Martin D, Swaney W, Bryant J, Castelli C, Robbins P, Parmiani G, Storkus WJ, Lotze MT. Tumor escape from immune recognition: lethal recurrent melanoma in a patient associated with downregulation of the peptide transporter protein TAP-1 and loss of expression of the immunodominant MART-1/Melan-A antigen. J Clin Invest. 1996; 98:1633–41. [PubMed: 8833913]

27. Yee C, Thompson JA, Byrd D, Riddell SR, Roche P, Celis E, Greenberg PD. Adoptive T cell therapy using antigen-specific CD8+ T cell clones for the treatment of patients with metastatic melanoma: in vivo persistence, migration, and antitumor effect of transferred T cells. Proc Natl Acad Sci U S A. 2002; 99:16168–73. [PubMed: 12427970]

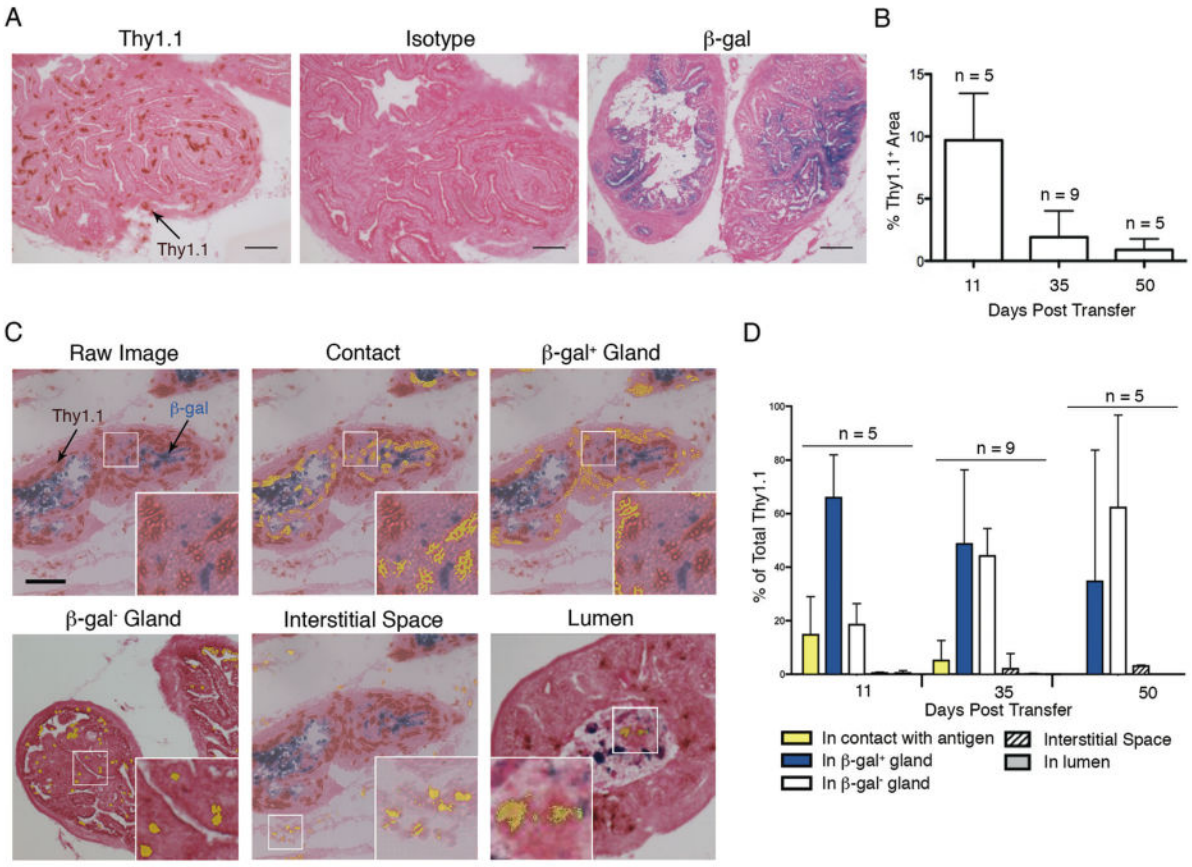

Figure 1.

Prostate infiltrating T cells gradually lose contact with antigen-expressing tumor cells. 2C T cells were adoptively transferred into TRP-SIY mice followed by WSN-SIY infection. Eleven, 35 and 50 dpt, prostate sections were stained with anti-Thy1.1 (brown), X-gal (blue) and eosin (red). A. Representative stains for Thy1.1 (left), isotype control (center) and β-gal (right) of prostate sections of TRP-SIY mice 11 dpt. Scale bars, 100μm. B-D. The areas of Thy1.1 and β-gal staining were quantified as described in the Materials and Methods. Shown are percentages (mean ± SD) of area within the prostate tissue that stain positive for Thy1.1$^+$ 2C T cells at indicated time point (B). Representative images of Thy1.1 and β-gal stains of prostate sections of a mouse 11 dpt (C). Thy1.1 staining was classified as either in contact with β-gal$^+$ cells (contact, highlighted in yellow), within a prostate gland containing β-gal$^+$ cells (β-gal$^+$ gland), within a prostate gland that does not contain β-gal staining (β-gal$^-$ gland), in the interglandular interstitial space (interstitial space), or within the lumen of the prostate gland (lumen). The boxed areas are shown in higher magnifications. Scale bars, 100μm and 30μm in low and high magnifications, respectively. The areas of Thy1.1 stain in each category were quantified and shown as percentages of total Thy1.1$^+$ area (mean ± SD) (D). The numbers of mice analyzed in each group for B and D are indicated.

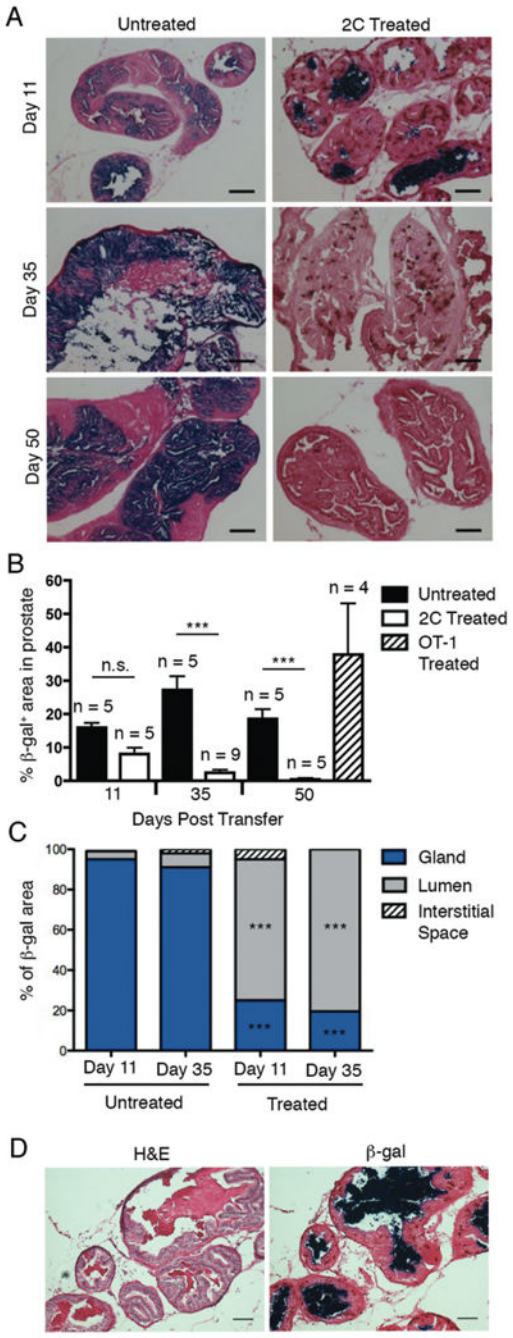

Figure 2.

Antigen positive cells are lost from 2C T cell-treated TRP-SIY prostates. Prostate sections from age-matched untreated and treated mice were stained for β-gal, Thy1.1 and eosin and both the β-gal and Thy1.1-stained areas were quantified. A. Representative images of staining for β-gal (blue) and Thy1.1 (brown) counterstained with eosin (red) of untreated mice and treated mice 11, 35 and 50 dpt. B. Percentages (mean ± SD) of $\beta\text{-gal}^{+}$ areas in the prostate section of untreated (black) and treated (open) mice at the indicated dpt. Some mice were transferred with OT-1 T cells and infected with WSN-SIIN virus and the percentage of

β-gal$^+$ area was quantified 50 dpt (dashed bar). The numbers of mice in each group are indicated. C. β-gal staining was classified as localizing to the gland (blue), lumen (grey) or interstitial space (dash) of the prostate sections from the same group of mice treated in B and expressed as an average percentage of total β-gal staining. D. Representative β-gal (left) ad H&E (left) staining of consecutive prostate sections from a mouse 11 dpt. Scale bars in both A and D, 100μm. ***p value of < 0.001 as compared to untreated group. n.s., not significant.

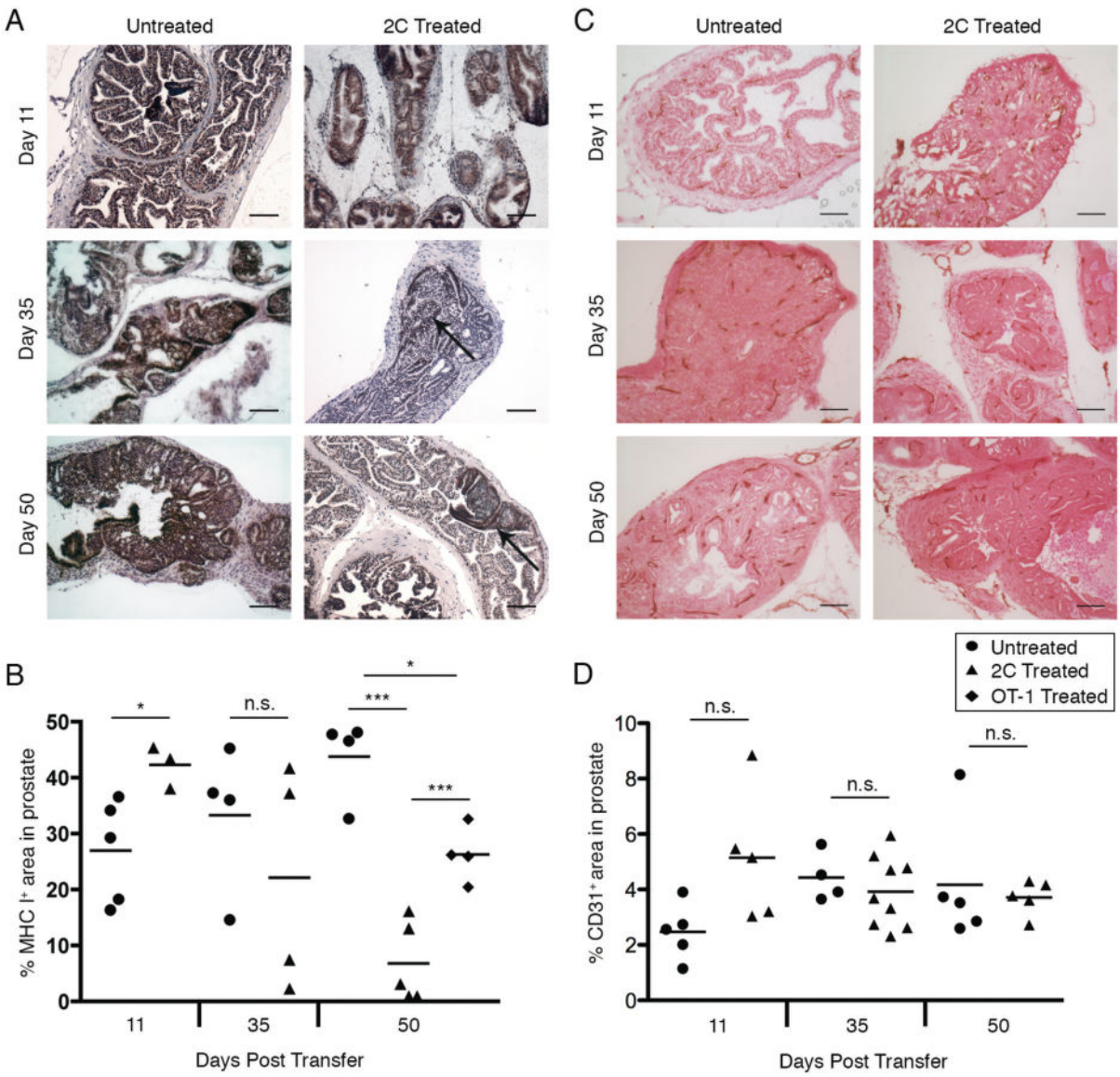

Figure 3.

MHC class I expression is reduced in 2C T cell treated prostates. A and B. Mice were treated as in Figure 2 and the 2C T cell treated prostate tissues and aged matched untreated control tissues (Untreated) were stained for MHC I (dark brown) and hematoxylin (light brown) and quantified. Representative staining of MHC I and hematoxylin from TRP-SIY prostate tissue at indicated time point with or without treatment (A). Percentages of area within the prostate tissue staining positive for MHC class I in 2C T cell treated (triangles), untreated (circles), or TRP-SIY mice receiving OT-1 T cells activated with WSN-SIIN virus (diamonds) at indicated time points (B). Each symbol represents one mouse. C and D. Prostate sections from age-matched untreated and 2C treated mice were stained for CD31 and eosin and the stained areas were quantified. Representative stains of CD31 (brown) and eosin (red) of untreated mice and treated mice 11, 35 and 50 dpt (C). Percentages (mean ± SD) of $CD31^+$ areas in the prostate section of untreated (circles) and 2C treated (triangles)

mice at the indicated dpt (D). Scale bars in A and C, 100μm. *p value of < 0.05; ***p value of < 0.001, n.s., not significant.

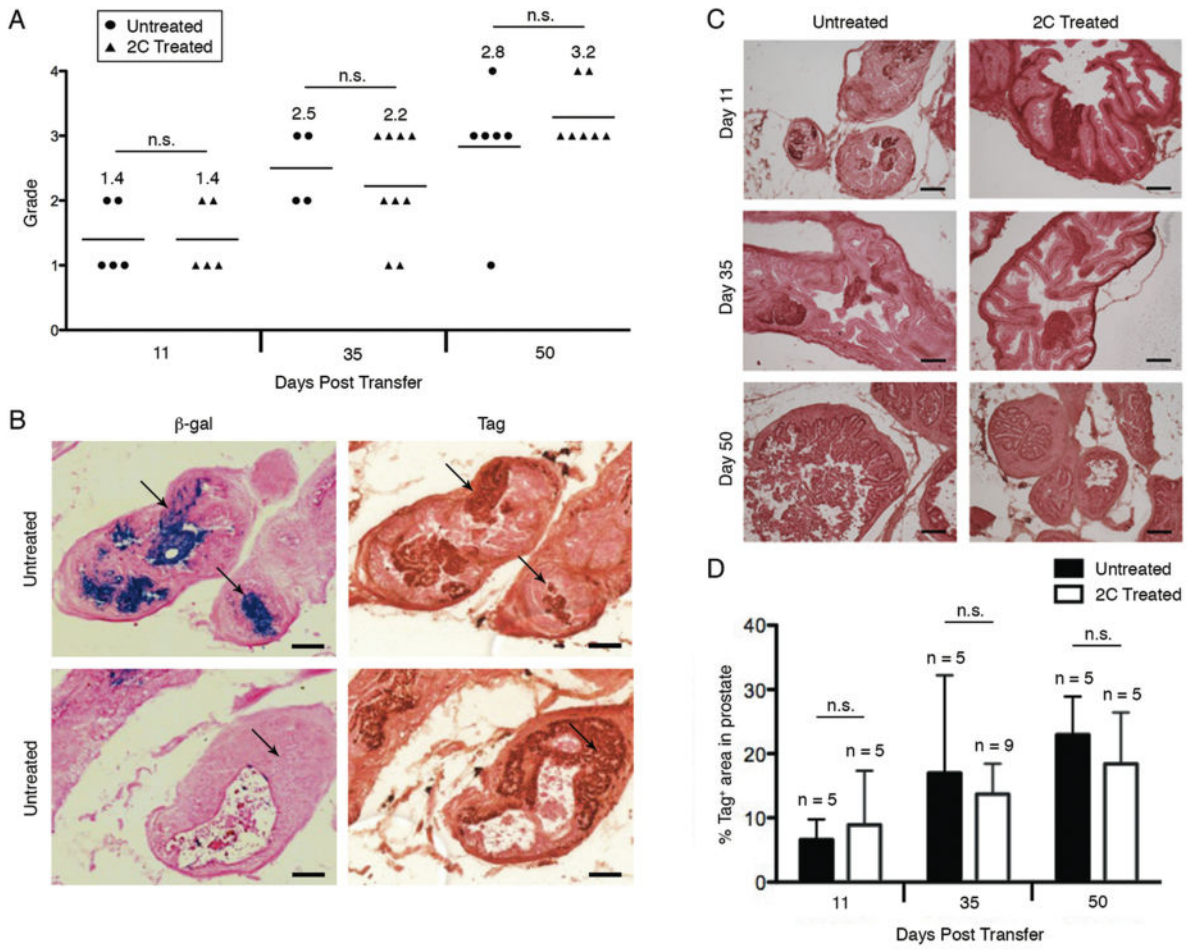

Figure 4.

2C T cell treatment does not affect tumor progression. A. Mice were treated as in Figure 2, prostate sections from both 2C T cell treated and age matched untreated mice were stained with H&E and graded (0, normal tissue; 1, proliferation with no invasion; 2, early invasion; 3, clear-cut invasion; 4, total replacement of organ). Shown are tumor grade at 11, 35, and 50 dpt. Each symbol represents one mouse. The numbers in parentheses indicate the average of tumor grade at each time point. B. Prostate sections from untreated TRP-SIY mice were stained for β-gal (blue), Tag (brown) and eosin (red). Representative images are shown for prostate sections from mice at 16 weeks of age. C and D. Mice were treated as in Figure 2, prostate sections from both 2C T cell treated and age matched untreated mice were stained for Tag (dark brown) and eosin (red). Shown are representative Tag staining of prostate sections from 2C treated mice at 11, 35 and 50 dpt and age-matched untreated mice (C). Percentages (mean ± SD) of Tag^+ areas in the prostate section of untreated and 2C treated mice at the indicated dpt (D). Scale bars in B and C: 100μm. n.s.: no statistical significance between groups.